Modeling of the Hydroentanglement Process

Ping Xiang[1], Andrey V. Kuznetsov[2], Abdelfattah Mohamed Seyam[1]

[1]North Carolina State University College of Textiles, Raleigh, North Carolina USA
[2] North Carolina State University, Department of Mechanical and Aerospace Engineering, Raleigh, North Carolina USA

Correspondence to:
Abdelfattah Mohamed Seyam, Ph.D. email: aseyam@tx.ncsu.edu

ABSTRACT

Mechanical performance of hydroentangled nonwovens is determined by the degree of the fiber entanglement, which depends on parameters of the fibers, fiberweb, forming surface, water jet and the process speed. This paper develops a computational fluid dynamics model of the hydroentanglement process. Extensive comparison with experimental data showed that the degree of fiber entanglement is linearly related to flow vorticity in the fiberweb, which is induced by impinging water jets. The fiberweb is modeled as a porous material of uniform porosity and the actual geometry of forming wires is accounted for in the model. Simulation results are compared with experimental data for a Perfojet ® sleeve and four woven forming surfaces. Additionally, the model is used to predict the effect of fiberweb thickness on the degree of fiber entanglement for different forming surfaces.

INTRODUCTION

Hydroentanglement is one of the fastest growing nonwoven fabric bonding technologies. In this process, a fabric is produced by subjecting a web of loose fibers to high-pressure fine water jets. The fiberweb is supported either by regularly spaced woven forming wires or other forming surface such as Perfojet® technology (sleeve with randomly distributed holes). As a result of the impact of the jets, the fibers entangle, forming an integrated web where fibers are held together by friction forces. The resulting fabric strength depends on the fiberweb properties (basis weight, thickness, etc.), fiber parameters (fiber diameter, bending modulus, etc.), forming wires geometry and jet parameters.

Most of hydroentanglement research has focused on experimental studies. Pourdeyhimi et al [1] experimentally investigated structure-process-property relations for hydroentangled nonwovens. Experimental research of Berkalp et al [2] examined the development of texture during this process as a function of water jets specific energy. Ghassemieh et al [3] used fast Fourier and Hough transformations in conjunction with two-dimensional scanning electron micrographs (SEM) images to evaluate fiber orientation and fiber length distribution in hydroentangled fabrics. The relationships between the micro-structural variables and mechanical fabric properties, such as strength and modulus, which can be used to estimate the degree of entanglement in hydroentangled fabrics, were also analyzed. However, experimental studies of this process are costly and elaborate and it is difficult to study the numerous combinations of fiberweb parameters, fiber properties, forming surface geometrical parameters, water jet variables and process speed in real-life experiments.

A number of theoretical studies of the hydroentanglement process were performed. Mao and Russell [4] defined the hydroentanglement intensity as the sum of the deflection depths of all fiber segments subjected to the impinging water jet impact. The hydroentanglement intensity depends on the applied energy, fiber dimensions and properties, as well as fiber deformations during the process. The effect of fiber rigidity on the hydroentanglement intensity was investigated and experimental data of fabric tensile strength for different fibers were found to be linearly correlated with the hydroentanglement intensity. Seyam et al [5] experimentally measured tensile strength and specific energy at low jet pressures, and correlated the results with jet drag forces, which were derived from a 2D mechanical cell model. However, the above theoretical methods were based on 2D mechanical properties of fibers and could not investigate the effect of other parameters, such as the process speed and fiberweb thickness, etc.

There is no currently available model that is capable of investigating the dynamics of the hydroentanglement process. The development of such a model is important because numerical simulations can help understanding the role of the water jets impact on the fiberweb and how the fiberweb is converted to an integrated nonwoven fabric with acceptable degree of fiber entanglement. This paper is aimed at developing such a model, which is then used to investigate the effect of hydroentanglement process parameters (such as the forming surface geometry, process speed, and jet pressure) on fabric strength and the efficiency of entanglement.

In this model, the realistic geometry of woven forming wires is considered, and the ricochet of water by forming surfaces is accounted for, which results in a thin fluid layer above the porous fiberweb. 3D simulations of water jets passing through the fiberweb and forming wires are performed and compared with experiments for the Perfojet ® and four woven forming surfaces.

MATHEMATICAL MODEL

This paper continues research of Xiang et al [6] in which the fiberweb and forming wires are modeled as two different layers of porous media. The present paper takes a step forward by taking into account the geometry of the forming surfaces. *Figure 1a* displays the schematic diagram of the hydroentanglement process and the computational domain. The *x*-axis is directed in the cross machine direction (CD), the *y*-axis is in the machine direction (MD), and the *z*-axis is

directed across the thickness of the fiberweb and the forming wires. The fiberweb is modeled as a porous layer with uniform porosity ϕ (the middle layer in *Figure 1a*, of thickness h_2). The forming wires layer (the lower layer in *Figure 1a*, of thickness h_3) is composted by solid wires and interstices between the wires *(see Figure 1b)*. The process is continuous, and the forming surface is moving in the MD. Only one manifold of the hydroentanglement process is investigated in this model.

After water hits the forming wires, part of it splashes back, so it is assumed that there is a thin fluid layer over the fiberweb. The portion of the injected water that is not splashed back goes all the way through the fluid layer (the upper layer in *Figure 1a*, of thickness h_1), the middle fiberweb layer, and the forming wires, and is finally evacuated.

In the hydroentanglement process, the impinging jets induce vortices within the fluid region, the fiberweb, and the interstices between the forming wires. The water vortices in the fiberweb cause the interaction between the impinging water and fibers in the fiberweb, involve fibers in vortices, align them along the water flow streamlines, and swirl them with the vortices. The rotational effect of fluid flow on a solid particle or a fiber is determined by flow vorticity. Shahcheraghi and Dwyer [7], for example, evaluated the rotation rate of a sphere in a flow field by one-half of the local flow vorticity at the sphere-center position. It is the rotational force on a fiber imposed by the water flow that causes the fiber to swirl and entangle with nearby fibers. It is therefore assumed that the degree of fiber entanglement is proportional to the average vorticity in the fiberweb region.

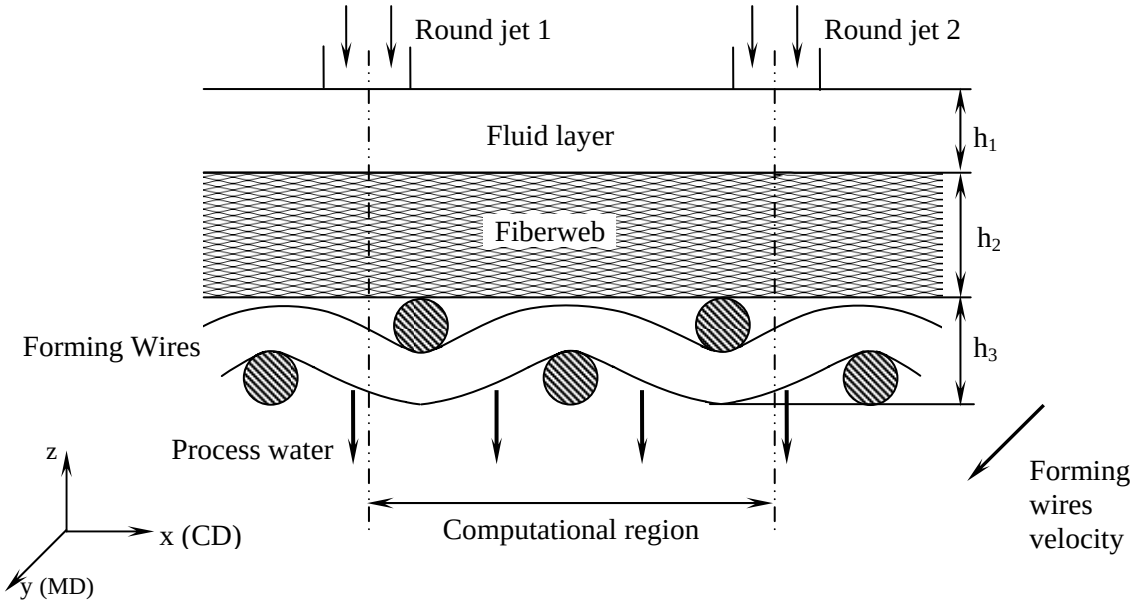

Figure 1a: Schematic diagram of the problem and the computational domain

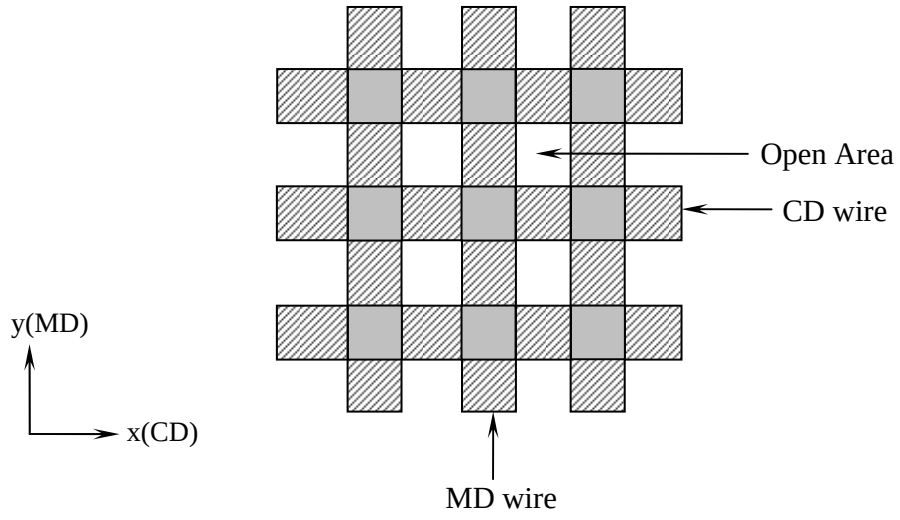

Figure 1b: Projection of forming wires on the MD-CD plane

Since the impinging jet velocity is very high, the flow in the fluid layer, porous fiberweb layer, and in the interstices between the forming wires *(see Figure 1a)* is turbulent. A turbulent flow model is used to simulate 3D flow in all three layers. The geometry of the computational domain for 3D simulations is shown in *Figure 2*, in which only two water jets are included. This is because all water jets in one manifold are identical and a manifold can be separated into many unit cells shown in *Figure 2*, in which the water flow field is similar and fiber entanglement simply accumulates when moving from one unit cell to the next.

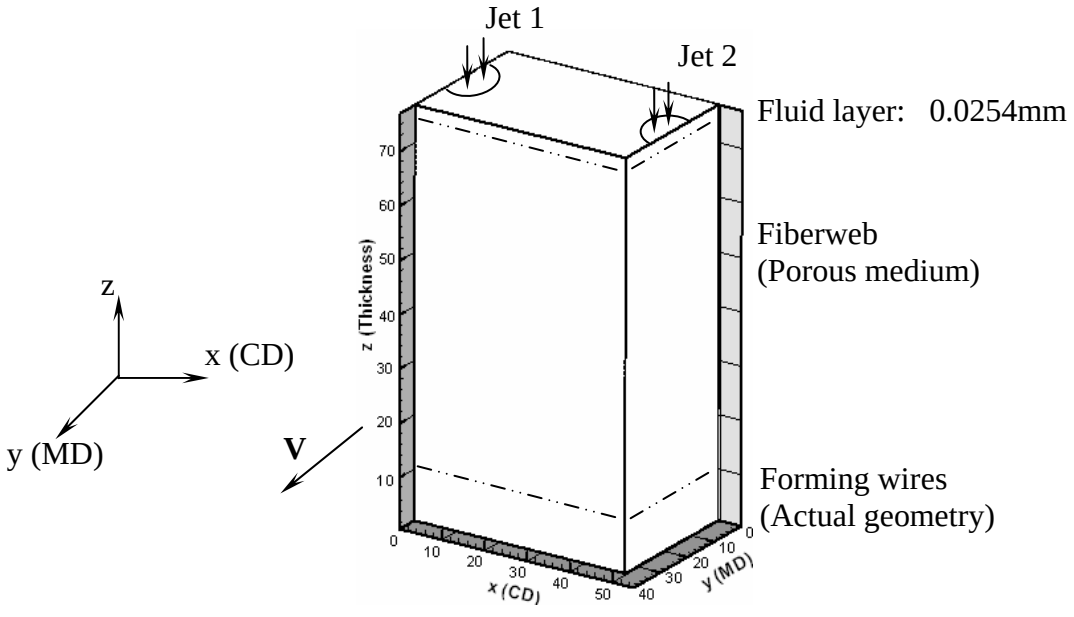

Figure 2: Computational domain for 3D simulations

RESULTS AND DISCUSSIONS

The results presented below validate the model. The model is also used to predict the influence of the fiberweb thickness on the degree of fiber entanglement.

Model validation

For model validation, simulation results are compared with experimental data of fiberwebs processed using a Perfojet® sleeve and four woven forming surfaces. To validate the assumption that the degree of fiber entanglement is proportional to the average vorticity in the fiberweb, the average vorticity in three different directions in the fiberweb layer is computed as $\frac{1}{T}\int\left[\iiint_V \left|(\nabla\times\mathbf{v})_i\right| \, dV \Big/ V\right]dt$, where $\nabla\times\mathbf{v}$ is the vorticity vector, $\left|(\nabla\times\mathbf{v})_i\right|$ is the absolute value of the i^{th} (i=x, y, z) component of the vorticity vector, V is the volume of the fiberweb within the computational domain *(see Figure 2)*, and T is the total impact time (calculated as the length of the computational domain in the MD over the velocity in the MD).

Perfojet® sleeve:

Experimental runs were conducted at Reiter Perfojet® labs in order to validate the model. A micro-perforated sleeve with 8% open area was used as a forming surface. The process speed was 0.5 m/s. The highly pressurized water jets impinging on the fiberweb have a typical diameter of 0.127mm, and the jet pressure was 5Mpa. There are 15.8 jets/cm (40 jets/ inch). Three fiberwebs are investigated whose parameters are listed in Table 1. The fiberwebs are made of 70% viscose and 30% polyester fibers. The basis weights shown in *Table 1* are averages of measured values.

Table 1: Parameters of the fiberweb processed using the Perfojet ® sleeve

Fiberweb	Basis Weight (g/m^2)	Thickness (mm)	Product density (g/cm^3)
1	34.3	0.517	0.0686
2	54.2	0.580	0.0934
3	76.9	0.695	0.1104

To compare with experimental results, simulations are performed to model experimental conditions as closely as possible. Since the Perfojet® sleeve is micro-perforated with a small open area (8%), in simulations it could be shown that 95% of the impinging water is reflected back by the sleeve. This is because it is assumed that the micro-perforated holes in the sleeve have cylindrical geometry with discharge coefficient of C_d = 0.62. It is also assumed that the water velocity does not change from the inlet to the exit of the holes in the sleeve.

For a perfojet sleeve with 8% open area, the ideal mass flow rate through the holes is $\dot{m}_{ideal} = 8\% \cdot \dot{m}_{total}$, where $\dot{m}_{total}$ is the total mass flow rate of the inlet water jets. So the actual

mass flow rate through the holes in the sleeve is $\dot{m}_{real} = \dot{m}_{ideal} \cdot C_d = 0.62 \cdot 8\% \cdot \dot{m}_{total} = 4.96\% \cdot \dot{m}_{total}$. Since all the water that didn't pass through the holes is reflected back, the mass flow rate of the reflected water is $\dot{m}_{reflection} = 1 - \dot{m}_{real} \cong 95\% \cdot \dot{m}_{total}$. Thus, 95% of impinged water is reflected back.

Since fabric tensile strength is used as a measure of the degree of fiber entanglement, the theoretically computed average vorticity in the fiberweb is compared with experimentally measured tensile strength for different fiberwebs [8]. The results for different fiberwebs in the MD and CD are shown in *Figure 3*. In this figure, the vorticity is calculated from the model and the tensile strength data were taken from reference 8.

The straight lines in *Figure 3* are the linear fit lines between the simulated and experimental results. The correlation coefficient, R, of the linear fit line for the results in the MD is 0.99407, while that for the results in the CD is 0.97641, which means that the correlation coefficients in both the machine and cross-machine directions are very close to unity. This indicated that there is a linear correlation between the fabric tensile strength and the average vorticity in the fiberweb. Since the fabric tensile strength is proportional to the degree of fiber entanglement, it is evident that the degree of fiber entanglement is linearly correlated to the average vorticity in the fiberweb, which validates the major assumption of this research.

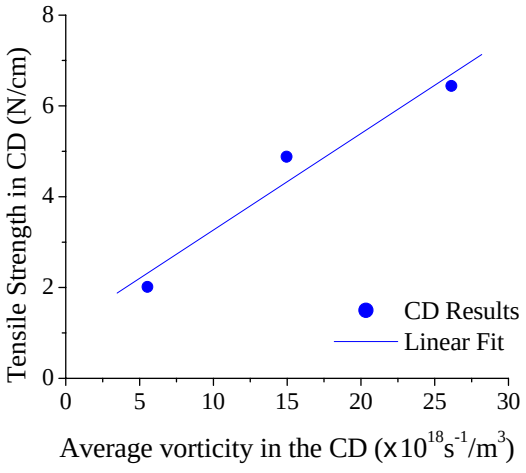

(a) Correlation in the CD (R=0.97641)

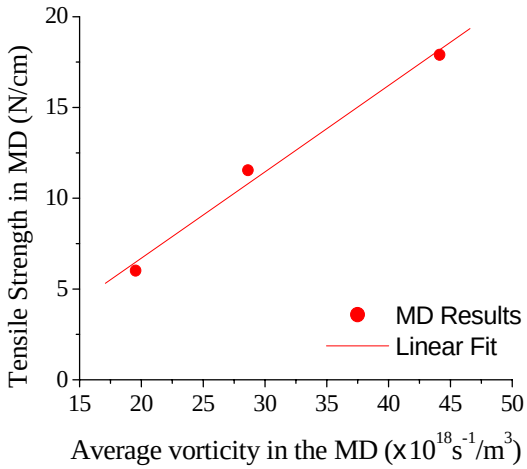

(b) Correlation in the MD (R=0.99407)

Figure 3: Experimental versus simulation results for the Perfojet ® sleeve

Woven forming wires:

In the experiments by Zheng [9], four different woven forming surfaces (with a plain wave structure) are investigated, whose geometrical parameters are listed in *Table 2*. Three of them are composed by wires with a round cross-section, and one is composed by wires with a rectangular cross-section. The process speed is 6.1 m/min in the MD for all runs. The water jets diameter is 0.127 mm, and there are 15.8 jets/cm (40 jets/ inch). Experiments are performed at six different

jet pressures: 3.45, 4.14, 4.83, 6.21, 7.58, and 8.96 MPa for each forming surface. The vacuum level is 4978 Pa. The carded and crosslapped fiberweb with a nominal basis weight of 50 g/m^2 is used for all runs. Actual basis weight was measured [9] and the tensile strength was prorated for 50 g/m^2 assuming linear relationship between tensile strength and basis weight to nullify the weight effect. The fiberweb is made of polyester fibers which have a linear density of 1.67 dtex, density of 1.38 g/cm^3, and diameter of 1.24×10^{-2} mm.

Table 2: Geometrical parameters of woven forming wires

Forming surface	Count (/inch)	MD wire diameter (mm)	CD wire Diameter (mm)	Open area, φ (%)	Wire cross-section shape	Thickness h_3 (mm)	Water re-flection rate Ri (%)
100 mesh	100 × 90	0.11	0.14	29%	Round	0.2794	11.36
36 mesh	36 × 27	0.40	0.40	25%	Round	0.6858	12.00
14 mesh	14 × 13	0.88×0.57	0.89	28%	Rectangle	1.3970	11.52
10 mesh	11 × 11	0.89	1.00	35%	Round	1.6510	10.40

Simulations are performed exactly for the same conditions as experiments. The measured thicknesses of the four woven forming surfaces are given in *Table 2*. For the woven forming surface, since it has a structure of interconnected wires and empty spaces between the wires, some of the inlet water is reflected back by the wires and the rest of water is evacuated through the interstices between the wires. Based on industry observations [10], it is assumed that 16% of the water that impinges on the wires is reflected back by the forming wires. Thus, the reflected portion of the water brought into the fiberweb by the jets is calculated as $Ri = 0.16\times(1-\varphi)$, where φ is the open area of the forming wires, which depends on geometry of the forming wires *(see Table 2).* In the present study, the migration of fibers into the interstices between the forming wires is neglected.

The average vorticity in the fiberweb for each forming surface is calculated at different water jet pressures for the comparison with experimental tensile strength results [9]. *Figure 4* gives the results for the "100 mesh" forming surface. From simulations presented in *Figure 4(a)* it is evident that the average vorticity in the fiberweb (hence, the fiber entanglement) increases with the jet pressure, which is consistent with the effect of the jet pressure on the fabric tensile strength *(Figure 4(b))* observed in experiments. The results presented in *Figures 4(a) and 4(b)* are used to produce *Figure 4(c)* that shows fabric tensile strength versus average vorticity in the fiberweb in the MD. A similar correlation in the CD is shown in *Figure 4(d).* The straight lines in *Figures 4(c) and 4(d)* are the linear fit lines between the simulated and experimental results in the MD and CD, respectively. The correlation coefficients of the linear fit lines in both the MD and CD are very close to unity (higher than 0.994).

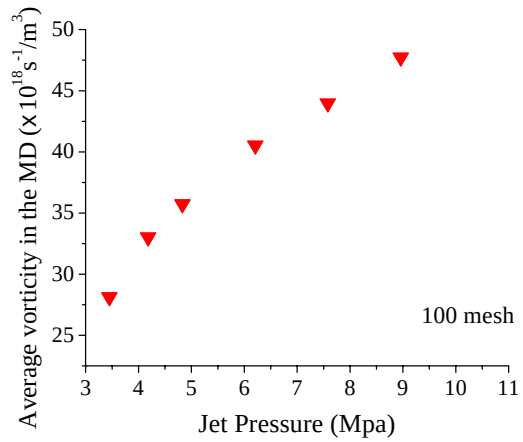

(a) Simulation results
at different jet pressures

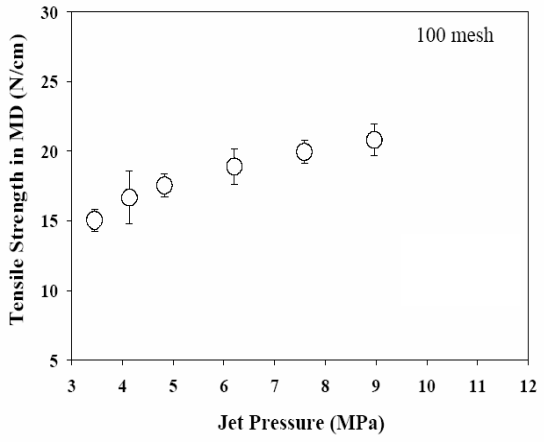

(b) Experimental results
at different jet pressures [9]

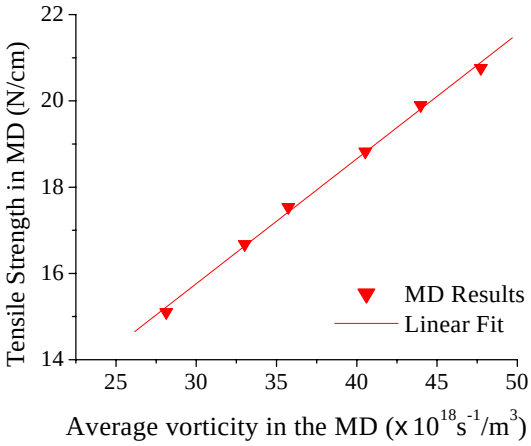

(c) Correlation in the MD (R=0.99864)

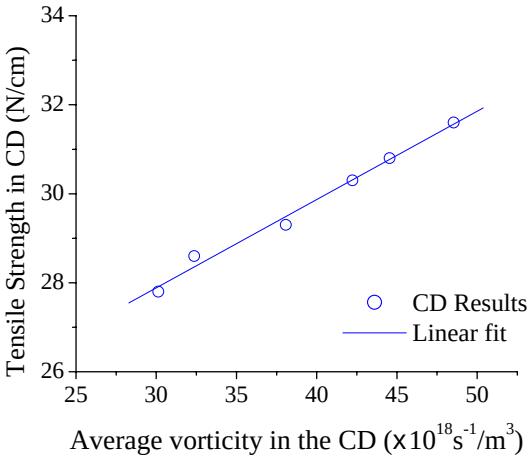

(d) Correlation in the CD (R=0.99458)

Figure 4: Comparison with experimental data for the "100 mesh" woven forming surface

Figures 5-7 display correlation results of the simulated average vorticity in the fiberweb in the MD and CD versus experimental tensile strength for the "36 mesh," "14 mesh," and "10 mesh" forming surfaces, respectively. The straight lines displayed in these figures are the linear fit lines between the simulated and experimental results. Similar to the "100 mesh" forming surface, it is also found that the correlation coefficients for these three different forming surfaces are close to unity (higher than 0.930), which indicates that there are linear correlations between the fabric tensile strength and the average vorticity in the fiberweb for these forming surfaces.

Since the fabric tensile strength is a measure of the degree of fiber entanglement, these results validate the major assumption of this research that the degree of fiber entanglement is linearly correlated with the average vorticity in the fiberweb for different woven forming wires (this assumption was validated for the Perfojet® sleeve in the previous section).

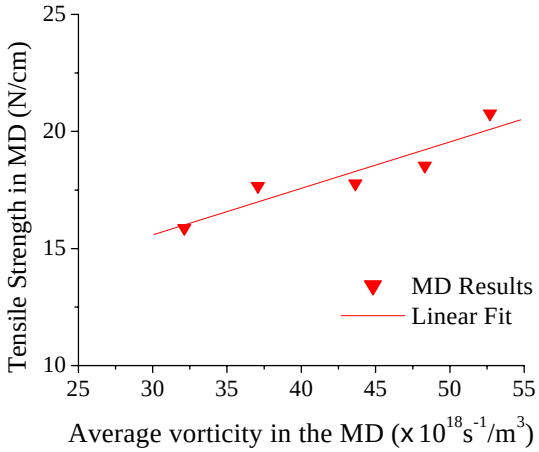

(a) Correlation in the MD (R=0.93134)

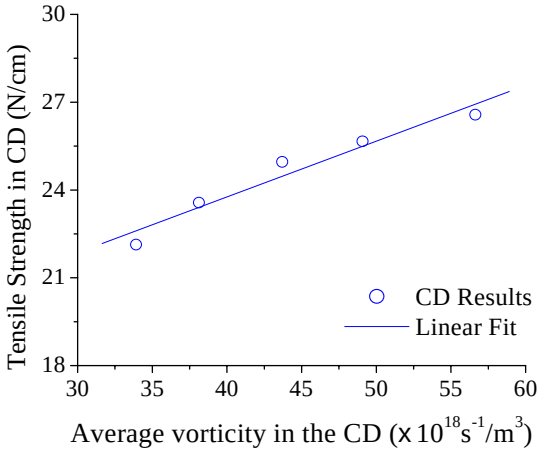

(b) Correlation in the CD (R=0.97332)

Figure 5: Comparison with experimental data for the "36 mesh" woven forming surface

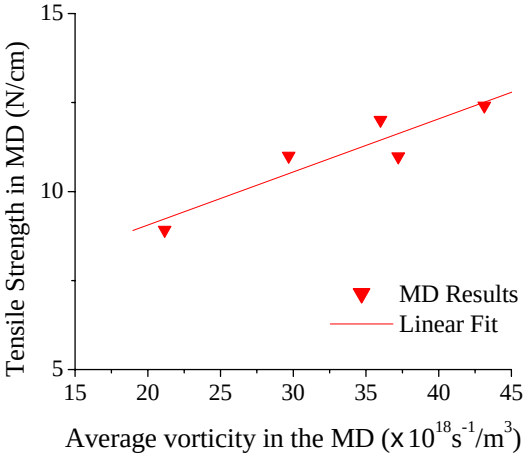

(a) Correlation in the MD (R=0.92295)

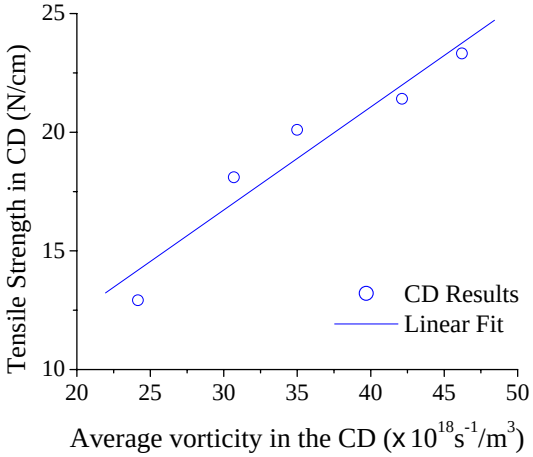

(b) Correlation in the CD (R=0.96166)

Figure 6: Comparison with experimental data for the "14 mesh" woven forming surface

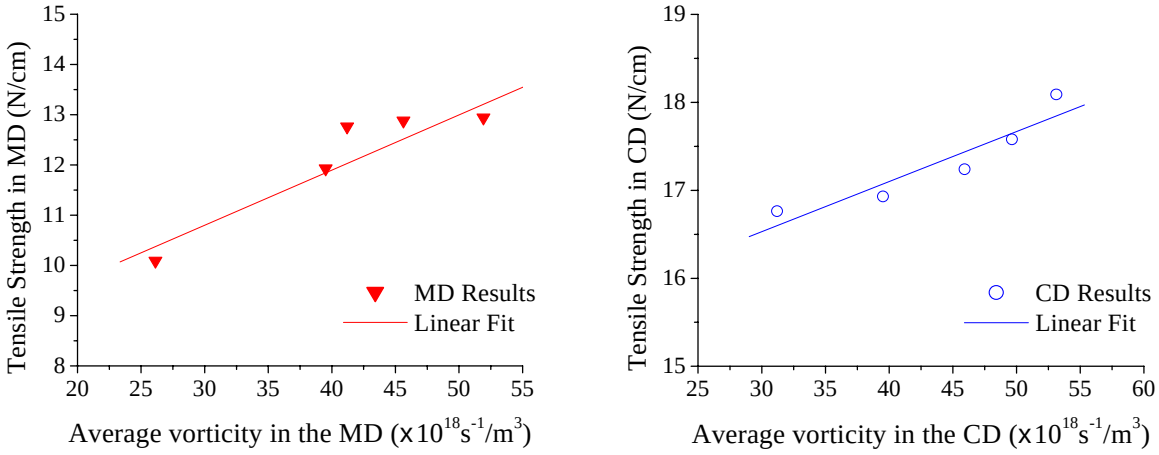

(a) Correlation in the MD (R=0.93581) (b) Correlation in the CD (R=0.93138)

Figure 7: Comparison with experimental data for the "10 mesh" woven forming surface

Comparing the correlation results in *Figures 5-7* with those in *Figure 4*, it is evident that the correlation coefficients for the "36 mesh," "14 mesh," and "10 mesh" forming surfaces are smaller than that for the "100 mesh" surface. This indicates that this model is more accurate for a fine mesh woven forming surface than a coarse one.

Since simulations are validated by extensive comparisons with experimental results, the model can now be used to compare entangling efficiencies for different conditions and determine optimal process parameters.

Influence of fiberweb thickness on fiber entanglement

Eight different fiberwebs with thicknesses ranging from 0.40 to 3.00 mm are used to investigate the effect of fiberweb thickness on fiber entanglement. All fiberwebs are carded and crosslapped with polyester fibers and have the same density as above experiments for woven forming wires in [9]. It is assumed that the fiberweb basis weight increases linearly with fiberweb thickness. Four different woven forming surfaces *(see Table 2)* are used. The water jets pressure is 20 MPa; other parameters of the water jets are the same as above experiments in [9].

Figures 8-11 depict the average vorticity in the fiberweb versus fiberweb thickness in the MD-CD plane, MD-fiberweb thickness direction (TD) plane, and CD-TD plane for four different forming wires. It is evident that the average vorticities in the fiberweb in all three planes decrease with the increase of the fiberweb thickness for the four different woven forming surfaces. This indicates that the fiberweb of the smallest thickness has the largest degree of fiber entanglement in a single manifold for a certain forming surface. It is also found that the average vorticity in the fiberweb remains almost unchanged when the fiberweb thickness is larger than 1.50 mm, which suggests that there is an asymptotic limit for the average vorticity in the fiberweb as the fiberweb thickness increases. This is because the kinetic energy of water jets

dissipates as water filters through the fiberweb. For the fiberweb of a large thickness, the kinetic energy completely dissipates in the upper portion of the fiberweb causing almost no entanglement in its lower portion. This means the process is only efficient for fiberwebs with a critical thickness (about 1.5 mm) in a single manifold.

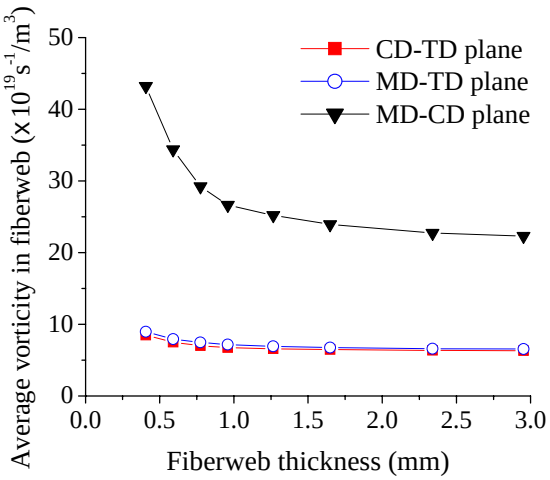

Figure 8: Effect of fiberweb thickness on the average vorticity in the fiberweb for the "100 mesh" woven forming surface

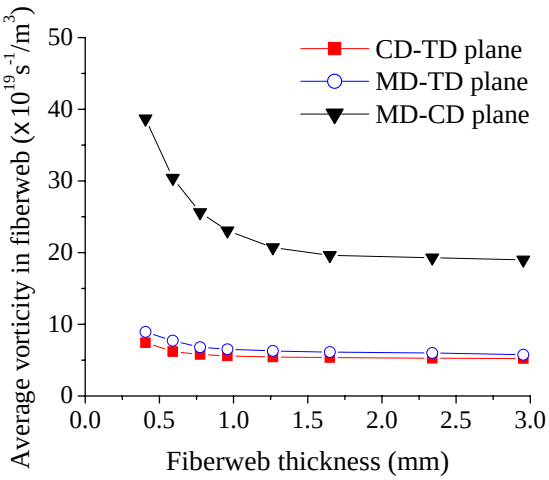

Figure 9: Effect of fiberweb thickness on the average vorticity in the fiberweb for the "36 mesh" woven forming surface

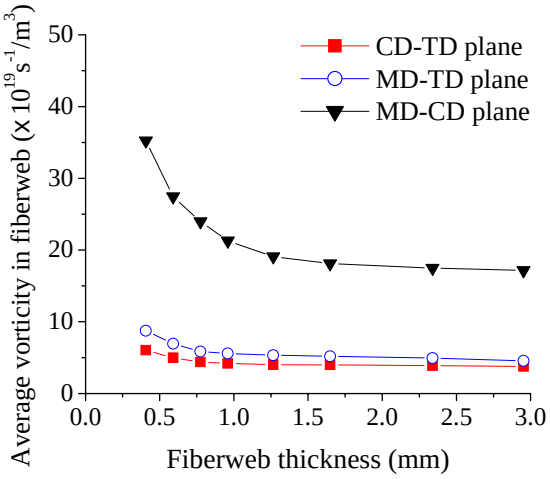

Figure 10: Effect of fiberweb thickness on the average vorticity in the fiberweb for the "14 mesh" woven forming surface

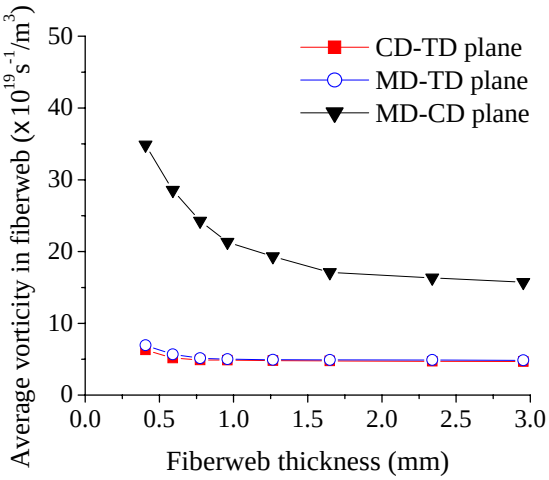

Figure 11: Effect of fiberweb thickness on the average vorticity in the fiberweb for the "10 mesh" woven forming surface

The results also show that the average vorticity in the fiberweb in the MD-CD plane is much higher than in the MD-TD and CD-TD planes. This means that the degree of fiber entanglement

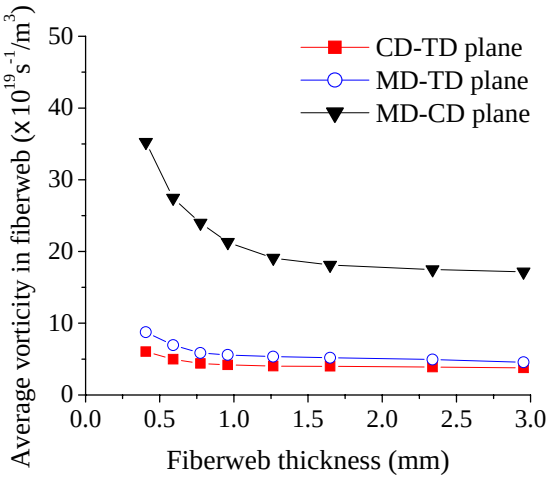

Figure 10: Effect of fiberweb thickness on the average vorticity in the fiberweb for the "14 mesh" woven forming surface

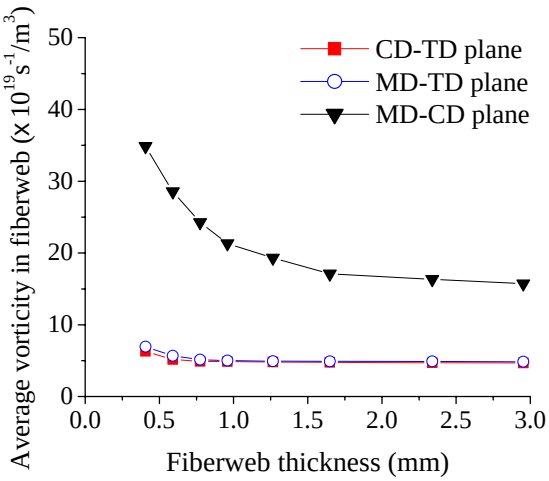

Figure 11: Effect of fiberweb thickness on the average vorticity in the fiberweb for the "10 mesh" woven forming surface

The results also show that the average vorticity in the fiberweb in the MD-CD plane is much higher than in the MD-TD and CD-TD planes. This means that the degree of fiber entanglement is the largest in the MD-CD plane; in other words, most of the fibers are entangled in the MD-CD plane.

Comparing the results presented in *Figures 8-11*, it is evident that the average vorticity in the fiberweb for the "100 mesh" forming surface is larger than the other three forming surfaces. This suggests that providing the open areas of different woven forming surfaces are about the same, fibers entangle better and the process is more efficient for a fine mesh forming surface.

Figure 12 shows contour lines depicting vorticity distributions in the MD-CD planes at different depths into the fiberweb for the fiberweb thickness of 3 mm. The *x* (CD) and *y* (MD) axis scales in the figures are dimensionless (to obtain a dimensional position, a dimensionless coordinate must be multiplied by 0.0127 mm). The values of vorticity are also dimensionless (to obtain a dimensional vorticity, a dimensionless vorticity must be multiplied by $15.75\times10^{6}\ s^{-1}$).

Figure 12 visualizes vortices induced by water jets in the fiberweb. The vorticity in the MD-CD plane decreases as the depth into the fiberweb increases, which results in fewer vortices in this plane. When the depth in the fiberweb is larger than 1.5mm, there are only few vortices in the MD-CD plane (Figure 12 (f)), and the fluid vorticity becomes so small the fluid does not have sufficient kinetic energy to entangle fibers. The visualization of the vorticity distribution demonstrates again that the critical fiberweb thickness is about 1.5 mm; up to this thickness fibers in the fiberweb are entangled efficiently in a single manifold.

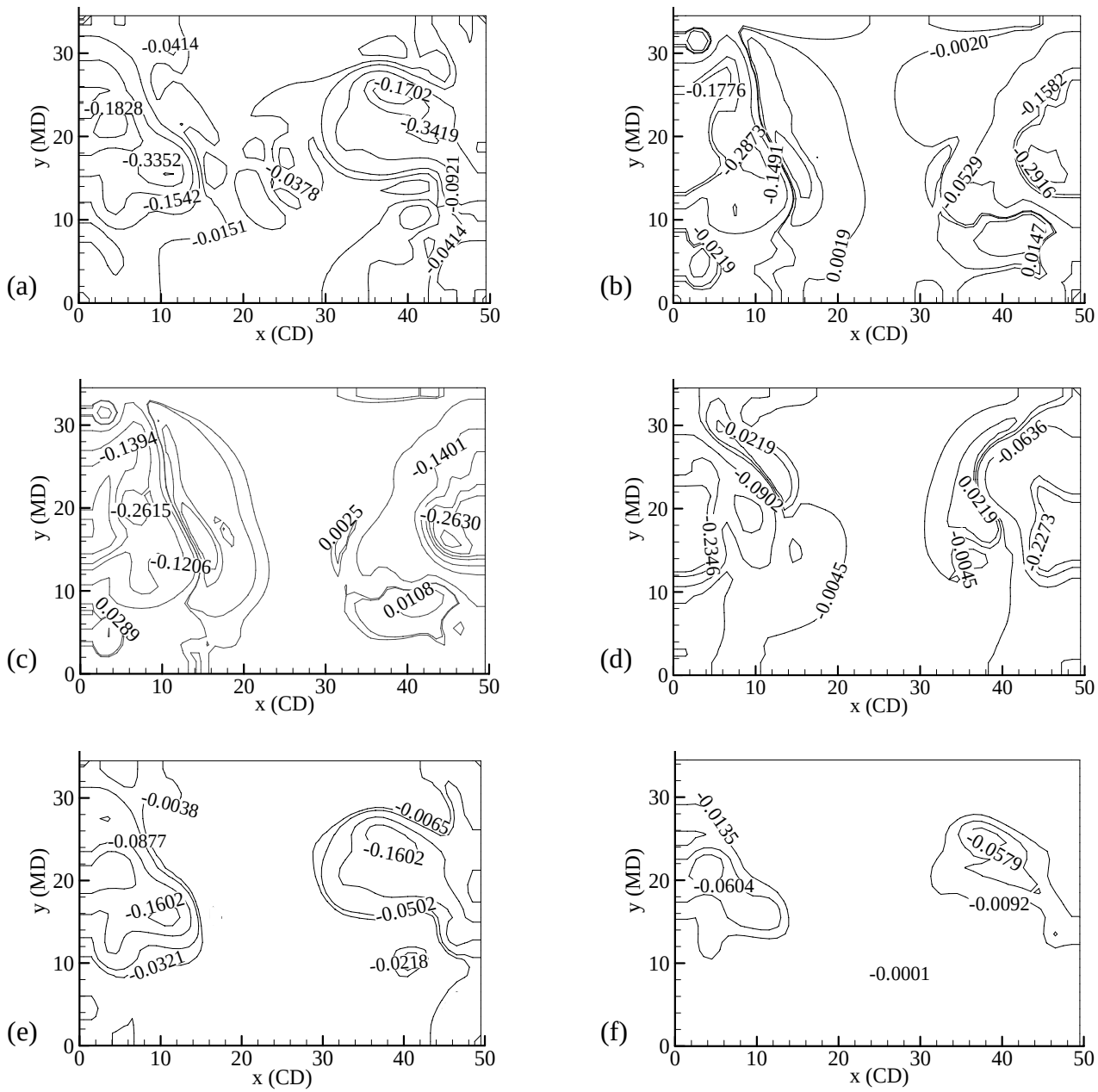

Figure 12: Vorticity distributions in the MD-CD planes at different depths into the fiberweb: (a) z=0.3 mm, (b) z=0.6 mm, (c) z=0.9 mm, (d) z=1.2 mm, (e) z=1.5 mm, (f) z=2.0 mm

CONCLUSIONS

A mathematical model describing the entangling effect of water jets impinging on the fiberweb and the forming wires has been developed. Since the rotational force on a fiber in water flow is

proportional to local flow vorticity, it is proposed to use the average vorticity in the fiberweb as a measure of the entangling effect produced by the impinging water jets.

The comparison of simulation results with experimental data for the Perfojet® and four woven forming surfaces validates this model's major assumption that the degree of the fiber entanglement is linearly proportional to the average vorticity in the fiberweb.

The model is applied to investigating the effect of fiberweb thickness on the degree of fiber entanglement. It is found that the average vorticity in the fiberweb decreases with the increase of fiberweb thickness. The results indicate that the average vorticity attains an asymptotic limit as the fiberweb thickness increases, which suggests there is a critical fiberweb thickness up to which the fibers entangle well and the process remains efficient. It is also found that most of the fibers in the fiberweb are entangled in the MD-CD plane, and that fibers entangle better on a fine mesh woven forming surface.

ACKNOWLEDGEMENTS

The support provided by the NCSU Nonwoven Cooperative Research Center of North Carolina State University is gratefully acknowledged. Helpful discussions with industry advisors to this project, C. Camelio, R. Holmes, F. Noëlle, and Dr. D. Shiffler, are greatly appreciated.

REFERENCES

1. Pourdeyhimi, B., Mintion A., Putnam, M. and Kim, H.S.; Structure-process- property relationships in hydroentangled nonwoven – Part 1: preliminary experimental observations, *International Nonwoven Journal*; vol. 13, no. 4, pp. 15-21, 2004

2. Berkalp, O.B., Pourdeyhimi, B. and Seyam, A.; Texture evolution in hydroentangled nonwovens, *International Nonwoven Journal*; vol. 12, pp. 28-35, 2003

3. Ghassemieh E., Acar M. and Versteeg H. K.; Microstructural analysis of non-woven fabrics using scanning electron microscopy and image processing. Part 2: application to hydroentangled fabrics, Proceedings of the Institution Mechanical Engineers, Part L, *Journal of Materials: Design and Applications*; vol. 216, No. 4, pp. 211-218, 2002

4. Mao N. and Russell S.J.; A framework for determining the bonding intensity in hydroentangled nonwoven fabrics, *Composites Science and Technology*; vol. 66, Issue 1, pp. 80-91, January 2006

5. Seyam, A. M., Shiffler D. A. and Zheng H.; An examination of the hydroentangling process variables, *International Nonwoven Journal*; vol. 14, no. 1, pp. 25-33, 2005

6. Xiang P., Kuznetsov A.V. and Seyam, A.; Simulation of fiber entanglement by modeling vorticity in water flow field, *Textile Research Journal*; 2006, In Press

7. Shahcheraghi N. and Dwyer H. A.; Moving and rotating sphere in the thermal entrance region of a heated pipe, Transactions of the ASME; vol. 122, pp. 336-344, 2000

8. RIETER Perfojet ®; Experimental results, 2006

9. Zheng, H.; The Impact of Input Energy, Fiber Properties, and Forming wires on the Performance of Hydroentangled Fabrics, Ph.D. Dissertation, North Carolina State University; pp. 89-97, 2003

10. Holmes, R.; Private communication, 2006

AUTHORS ADDRESSES

Abdelfattah Mohamed Seyam, Ph.D., Ping Xiang, M.S
North Carolina State University
College of Textiles
2401 Research Drive
Raleigh, North Carolina 27695-8301 USA

Andrey V. Kuznetsov, Ph,D.
North Carolina State University
Department of Mechanical and Aerospace Engineering
2401 Research Drive
Raleigh, North Carolina 27695-8301 USA